Naval Research Laboratory

Washington, DC 20375-5320

NRL/MR/6120--20-10,075

Electrospun Multifunctional Composite Fibers for Improved Warfighter Insect Protection

Jeffrey Lundin

Materials Chemistry Branch
Chemistry Division

Justin Ryan

NRC Post-Doctoral Fellow
Chemistry Division

Riccardo Casalini

Materials Chemistry Branch
Chemistry Division

Joshua Orlicki

Polymers Branch
CCDC U.S. Army Research Laboratory
Aberdeen Proving Ground, MD

July 13, 2020

REPORT DOCUMENTATION PAGE

Form Approved
OMB No. 0704-0188

1. REPORT DATE *(DD-MM-YYYY)*	**2. REPORT TYPE**	**3. DATES COVERED** *(From - To)*
13-07-2020	NRL Memorandum Report	Mar 2019 – Mar 2020

4. TITLE AND SUBTITLE

Electrospun Multifunctional Composite Fibers for Improved Warfighter Insect Protection

5a. CONTRACT NUMBER

5b. GRANT NUMBER

5c. PROGRAM ELEMENT NUMBER
0603716D8Z

6. AUTHOR(S)

Jeffrey G. Lundin, Justin J. Ryan, Riccardo Casalini, and Joshua Orlicki

5d. PROJECT NUMBER

5e. TASK NUMBER

5f. WORK UNIT NUMBER
9512

7. PERFORMING ORGANIZATION NAME(S) AND ADDRESS(ES)

Naval Research Laboratory
4555 Overlook Avenue, SW
Washington, DC 20375-5320

US Army Research Laboratory
Aberdeen Proving Grounds, MD 21005

8. PERFORMING ORGANIZATION REPORT NUMBER

NRL/MR/6120--20-10,075

9. SPONSORING / MONITORING AGENCY NAME(S) AND ADDRESS(ES)

Strategic Environmental Research and Development
Program SERDP
4800 Mark Center Dr.
Alexandria, VA 22350

10. SPONSOR / MONITOR'S ACRONYM(S)

SERDP

11. SPONSOR / MONITOR'S REPORT NUMBER(S)
WP19-1187

12. DISTRIBUTION / AVAILABILITY STATEMENT

DISTRIBUTION STATEMENT A: Approved for public release; distribution is unlimited.

13. SUPPLEMENTARY NOTES

14. ABSTRACT

Conventional insect repellent treatments for fibers, fabrics, and garments suffer from limited durability to repeated laundering and, depending on the insecticide, potential irritation or toxicity. In this work, monofilament and coaxial electrospinning were employed to control the composition of hierarchically-structured functional micro- to nano-scale fibers for tunable insect repellent release. Specifically, picaridin was incorporated into Nylon-6,6 nanofibers for the first time via monofilament and coaxial electrospinning, in which the sheath component has potential to protect additives in the core for more durable fabrics and act as a diffusion barrier for extended release applications. The size and morphology of nylon fibers were unaffected by picaridin incorporation, even at loading concentrations up to 50 wt%. Picaridin release kinetics were largely dependent on loading concentration and temperature, as picaridin-nylon intermolecular interactions were minimal affording diffusion based release. Importantly, coaxial fibers composed of nylon-picaridin core surrounded by a nylon sheath demonstrated altered release kinetics demonstrating the capability to further tune behavior.

15. SUBJECT TERMS

Fibers
Insect repellents
Electrospinning
Textiles

16. SECURITY CLASSIFICATION OF:			**17. LIMITATION OF ABSTRACT**	**18. NUMBER OF PAGES**	**19a. NAME OF RESPONSIBLE PERSON**
a. REPORT	**b. ABSTRACT**	**c. THIS PAGE**			Jeffrey G. Lundin
Unclassified Unlimited	Unclassified Unlimited	Unclassified Unlimited	Unclassified Unlimited	41	**19b. TELEPHONE NUMBER** *(include area code)* (202) 767-2529

Standard Form 298 (Rev. 8-98)
Prescribed by ANSI Std. Z39.18

This page intentionally left blank.

Table of Contents

Table of Figures

Abbreviations

ARL	Army Research Laboratory
ATR-FTIR	Attenuated Total Reflectance Fourier Transform Infrared
DEET	*N,N*-Diethyl-*meta*-toluamide
DSC	Differential Scanning Calorimetry
E_a	Activation Energy
FA	Formic Acid
GC-MS	Gas Chromatograph / Mass Spectroscopy
IR	Infrared
ND	Nylon/DEET composite
NP	Nylon/Picaridin composite
NRL─DC	Naval Research Laboratory, Washington D.C.
SEM	Scanning Electron Microscopy
TGA	Thermogravimetric Analysis
wt%	Weight Percent

Keywords

Electrospinning, fibers, repellents, coaxial, multifunctional composites

Acknowledgements

In support of this joint initiative, the authors wish to thank the following parties:

Dr. Robin Nissan from the SERDP Program Office for financial support; the Office of Naval Research and the US Naval Research Laboratory.

1. Executive Summary

1.1. Introduction and Objectives

Fabrics and garments that exhibit similar feel of existing uniform fabrics, while also exhibiting superior performance via the incorporation of safer insect repellents (i.e. picaridin) have potential to greatly reduce the environmental and toxic burden of functional textiles. By improving the durability of the insect repellent fibers to laundering and degradation due to normal wear, sustainability can be improved since textiles will exhibit longer lifecycles in the field. The objective of this research was to develop novel multifunctional fibers containing environmentally friendly low toxicity insect repellents intelligently localized in textile-relevant polymeric fibers, such as nylon, with core-shell morphology via coaxial electrospinning. Coaxial electrospinning afforded the potential to create hierarchically-structured functional micro- to nano-scale fibers by control over the composition of specific areas of the fiber (core vs. surface).

1.2. Technical Approach

The general approach of this work employed coaxial electrospinning to physically embed active additives into the core of textile fibers. First, insect repellents were uniformly distributed through monofilament Nylon fibers and then incorporated separately into the core of nylon, by coaxially electrospinning. Coaxial electrospinning afforded control over the design of the polymer shell (Figure 1) to tune the permeability of the polymer fiber to the additive in the core and control its release. This is critical for the insect repellent application, in which the release should be slowly occurring during the lifetime of the garments. Thorough material characterization was performed to evaluate fiber designs and compare the release of two insect repellents, DEET and picaridin.

Manuscript approved April 22, 2020.

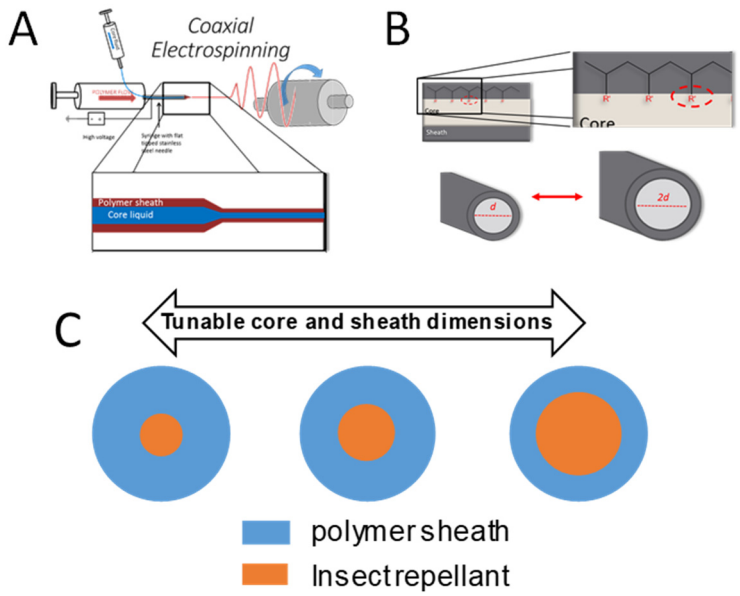

Figure 1. Schematics of A) formation of aligned nano-/micro-fibers by coaxial electrospinning, B) cross-sections of core/sheath fiber demonstrating control of interfacial chemistry and diameter, and C) cross-section of fiber structures demonstrating conceptual approach to control release rate and optimize lifetime

1.3. Results

Repellent nanofibers composed of picaridin in Nylon-6,6 were successfully developed. Electrospinning proved successful to demonstrate blends and coaxial nylon fiber designs that exhibited tunable and delayed release performance. The results described herein represent a significant proof of concept of the validity of the technical approach and identifies significant potential for the development of durable insect repellent textiles. Fabrication of electrospun repellent fibers containing the insect repellent picaridin was demonstrated and thermogravimetric analysis (TGA) was most effective in demonstrating the tunable release of repellent. A comparison of monofilament and coaxial structures provided evidence of another design tool by which to encapsulate volatile liquids and simultaneously control their release through fabrication inputs. TGA profiles of monofilament repellent fibers elucidated information on activation energies and

release kinetics that cemented the importance of environmental conditions (*i.e.* ambient temperature, humidity) important to designing high durability fibers for improved warfighter uniforms.

Coaxial fibers demonstrated the ability to withstand high temperatures by physically limiting diffusion of the repellent-rich core through the fiber, further confirming the durability and performance of a coaxial fiber and its advantage compared to traditional monofilament fibers and textiles.

1.4. Benefits

Electrospinning demonstrated the ability to prototype multifunctional composites that can be easily implemented and transferred to commercial production facilities. The ability to encapsulate volatile repellents like DEET and picaridin in textile-relevant materials increases the likelihood of deploying such systems across a wide range of battlespace environments. Thermal analysis was the most effective in characterizing and iterating the design of such fibers for generating platforms with tunable release profiles via bottom-up approach. Calculation of activation energies via Arrhenius equations provided further insight into small-molecule diffusion, impacting the design of electrospun repellent fibers. Scanning electron microscopy demonstrated that monofilament fiber morphology was largely unaffected by repellent incorporation, even at extremely high loadings. Similarly, coaxial morphology was largely independent of repellent loading, though at very high loading levels, more defects in fiber morphology were identified, which would be expected to compromise mechanical integrity. Further investigations of these systems would focus on optimization of thermomechanical performance as related to both morphology and composition of the insect repellent fibers. Fourier transform infrared spectroscopy

demonstrated that even though no specific binding occurred between the relatively polar repellents and Nylon, physical encapsulation provided an adequate barrier that enabled release of repellent over very long times compared to more traditional topical approaches. This suggests that there is opportunity for further research to investigate more highly interacting systems, through exploitation of specific binding (*i.e.* ionic, H-bonding, etc.) to create ultra-durable, long-lasting multifunctional textiles. Additionally, because of the simplicity of electrospinning, this fabrication approach lends itself to potential implementation towards additional systems of interest including flame retardants, energetics, and supported catalysts. The flexibility afforded by electrospinning provides the opportunity for the generation of a library of multifunctional fibers with different additives, chemistries, and physical properties. Individual fibers may be tuned to encapsulate varying functionalities and at different concentrations; or, monofunctional fibers may be blended to form multifunctional fibers or yarns depending upon the use case (Figure 2).

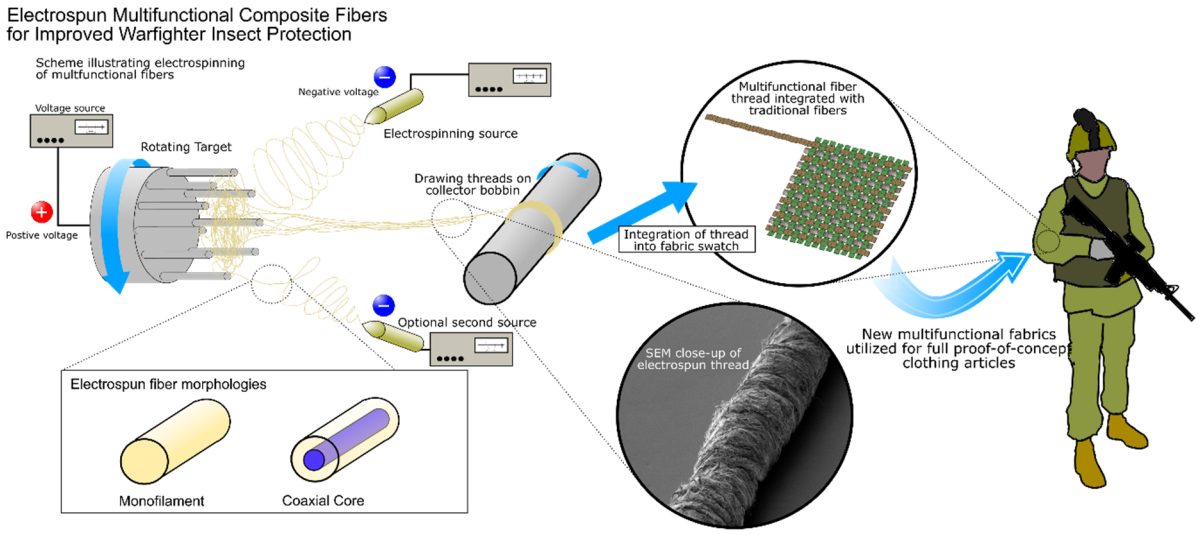

Figure 2. Scheme depicting a potential pathway to scale multi-functional coaxial electrospun fibers into threads and woven into textiles for uniform applications

2. Background

Biting arthropods (e.g. mosquitos and ticks) not only present incessant irritation, but also function as significant vectors that spread disease among populations. Other than physical barriers such as mosquito netting, the most successful method to reduce insect bites has been the application of chemical-based repellents, often aerosol-type spray or topical lotion, that deter insects from a particular area or person.[1] Currently, there are several repellents approved by the FDA, of which *N,N*-Diethyl-*meta*-toluamide (DEET) is the most popular, followed by 1-(1-Methylpropoxycarbonyl)-2-(2-hydroxyethyl)piperidine (Picaridin), Ethyl *N*-acetyl-*N*-butyl-β-alaninate (IR3535), and other essential oils.[2] The repellent mechanism for each insect repellent differs. For example, DEET has been proposed to repel insects through multiple mechanisms, both through avoidance via olfactory binding and as an olfactory confusant by masking the host's odors.[3-4] Picaridin interacts with similar olfactory binding sites as DEET due to structural similarity, but also binds to other novel sites providing a slightly different mode of action.[5] In contrast, (3-phenoxyphenyl)methyl-3-(2,2-dichloroethenyl)-2,2-dimethylcyclopropane-1-carboxylate (Permethrin) is an effective insecticide that kills insects and ticks through neurotoxic means.[1] Compared to DEET, picaridin exhibits comparable repellency against both mosquitos and ticks,[6-7] yet picaridin has lower toxicity, less skin irritation, better compatibility with plastics, and slightly longer duration.[8]

An inherent limitation to insect repellents is their finite efficacy time due to evaporation of the liquid-based repellents. A common strategy to combat this limitation has been to control the repellent release rate and/or to provide a reservoir from which to draw additional repellent. Polyester fabrics were modified to exhibit repellency by modification with complexed DEET with a cyclodextrin and grafting through an anhydride that demonstrated improved resiliency to

washing with detergents.[9] A common approach is to mix the insect repellent directly into a polymer solution prior to production into a fiber or coating. For example, DEET was incorporated into polylactic acid fibers via coextrusion for potential textile applications, where DEET reduced mechanical properties of the PLA fibers while only contributing minor repellent effects.[10] Modified polymer coatings are also employed to impart insect repellents to existing materials. Recently, applications of DEET and IR3535 polymer-based coatings to netting were demonstrated to provide a physical barrier that also exhibited repellent properties that lasted up to 29 weeks.[11] Another approach is the incorporation of particles, or capsules, that contain insect repellent, which are then imparted onto a material to provide long-term repellency with improved water resistance. For example, microcapsules composed of picaridin encapsulated with commercial antibacterial and antifungal microbiocide polymer demonstrated significant stability in water and maintained efficacious levels of insect repellency when adsorbed onto nylon-cotton blended fabric.[12] Nanospheres containing DEET fabricated from miniemulsion polymerization resulted in sustained and temperature dependent release kinetics.[13] Furthermore, covalent attachment of DEET to Nylon 6 via dye modification demonstrated some insect repellent activity, though chemical modification of DEET reduced efficacy in some cases.[14] While each of these approaches were effective, a material (i.e. fiber) with insect repellent incorporated directly into it at the manufacturing stage would reduce the complexity of many of the coating and particle impregnation methods.

Electrospinning is a facile method for the fabrication of micro- and nano-scale polymer fibers.[15] Recently, electrospinning has shown broad capability to generate a variety of polymer fibers of single and composite composition.[16-18] Electrospun polylactic acid fibers containing DEET at concentrations exceeding 50 wt% demonstrated uniform fiber morphology and delayed

evaporation of DEET as compared to the neat repellent.[19-20] Furthermore, electrospun pyromellitic dianhydride-cyclodextrin-based fibers were loaded with DEET and shown to maintain fiber morphology, as well as provide increased release times.[21] Interestingly, coaxial electrospinning provides yet another layer of control,[22] where fibers with core-sheath morphology are fabricated to contain different composition in the center of a polymer micro-/nano-fiber, including liquids[23-24] and bioactive compounds.[25] Coaxial electrospinning is a convenient and inexpensive method to control morphology and composition, the designs of which can be applied to large-scale fabrication techniques, such as melt extrusion or spinning, for scale-up. Recently, melt spinning was used to fabricate bicomponent fibers composed of a DEET and poly(ethylene-co-vinyl acetate) core surrounding by a HDPE sheath that demonstrated long-term efficacy following numerous cold water washes.[26] Such fibers have not yet been demonstrated using picaridin with traditional textile relevant polymers.

Compared to a monofilament construction, the sheath component of a coaxial fiber would aid in protecting additives in the core for more durable fabrics and act as a diffusion barrier for extended release applications. The sheath material offers the opportunity to tune diffusion rates based on composition, and afford additional control through the modulation of thickness. In this work, picaridin was incorporated into Nylon-6,6 nanofibers for the first time via monofilament and coaxial electrospinning. The effects of fiber composition on fiber morphology and release kinetics on monofilament fibers were investigated. Coaxial fibers composed of Picardin loaded Nylon core surrounded by an unloaded Nylon sheath were fabricated and demonstrated altered release kinetics. Despite the many benefits of picaridin over DEET, there have been no studies to date on the effects of picaridin loading in fibers through electrospinning and its effects on morphology, structure, and release. This represents a facile method for generating defect-free,

insect repellent fibers composed of a textile relevant polymer that can be tuned through traditional electrospinning methods or applied to conventional fiber fabrication methods.

3. Materials & Methods

Materials. Pelletized nylon-6,6 and *N*,*N*-Diethyl-3-methylbenzamide (DEET, 97%) were purchased from Sigma-Aldrich (St. Louis, MO), while formic acid (88%) and picaridin (98%) were purchased from Fisher Scientific and Combi-Blocks, respectively, and used without further purification.

Electrospinning. All electrospun nanofibers were prepared from homogenous solutions with formic acid as solvent and a nylon-6,6 concentration of 12.5 wt%. In the case of composite fibers, a predetermined amount of insect repellent was incorporated into the nylon-6,6 solutions to achieve nominal solution concentrations of 10, 30, and 50 wt% repellent with respect to nylon-6,6, solids content, designated for picaridin composites as NP10, NP30, and NP50, respectively, and DEET composites as ND10, ND30, and ND50, respectively.

Monofilament Electrospinning. Electrospinning was performed on a custom-built platform equipped with a syringe pump (New Era Pump Systems) containing a filled 12 mL syringe attached to a 22 G needle (D = 0.020 in). Fibers were spun at 15 kV onto a grounded plate at a constant working distance of 10 cm and a flow rate of 15 μL/min.

Coaxial Electrospinning. The same procedure was used for coaxial spinning as for monofilament spinning, however, a coaxial needle (Rame Hart, Succasunna, NJ, inner needle i.d./o.d. = 0.411/0.711 mm, outer needle i.d./o.d. = 2.16/2.77 mm) was utilized where the outer needle solution was a pure (no repellent) Nylon-6,6 solution (12.5% in formic acid) and the inner needle solution was a NP50 solution. To alter the fiber composition, the inner needle flow rate was

systematically varied and set at 1, 5, 10, and 15 μL/min (15-1, 15-5, 15-10, 15-15, respectively), while the outer needle flow rate was held constant at 15 μL/min for all experiments. For both monofilament and coaxial experiments, electrospun nanofibers were allowed to dry at ambient conditions for 24 h to ensure any residual solvent was removed.

Scanning Electron Microscopy. Images of nanofiber morphology were obtained by scanning electron microscopy (SEM) on a JEOL JSM-7600F field emission SEM (Peabody, MA) at an operating voltage of 5 kV. Samples were sputter coated with least 3 nm of gold prior to SEM analysis using a Cressington 108 auto sputter coater equipped with a MTM20 thickness controller. Fiber diameters were measured from SEM images using ImageJ software ($n \geq 50$).

Thermal Analysis. Analysis of fiber composition and release kinetics were characterized by thermogravimetric analysis (TGA) on a TA Instruments Discovery TGA using platinum plans. Heating ramps were performed at a heating rate of 10 °C/min to 600 °C. Isothermal measurements were performed in nitrogen atmosphere at 60, 80, and 100 °C for 5 h. Glass transition temperature (T_g) and thermal behavior were determined on a TA Instruments Discovery Differential Scanning Calorimeter (DSC). Temperature ramps were performed from -50 °C to 300 °C at a rate of 10 °C/min.

Fourier Transform Infrared Spectroscopy. Structural characterization of electrospun nanofibers was investigated through attenuated total reflectance Fourier transform infrared (ATR-FTIR) spectra were using a Thermo Scientific Nicolet iS50-FT-IR spectrometer equipped with an iS50 ATR attachment and Ge crystal. Background and sample spectra consisted of 128 scans

averaged together with 4 cm^{-1} resolution at a scanner velocity of 10 kHz.

4. Results and Discussion – DEET Fibers

Physical incorporation of the liquid repellent DEET into solutions of Nylon-6,6 in formic acid is expected to behave as a non-volatile diluent, homogenously distributed throughout the fiber matrix during the electrospinning process, resulting in a composition-dependent fiber morphology. After confirmation that Nylon/DEET (ND) solutions were miscible over the composition range of interest, fiber morphology was analyzed.

To facilitate discussion and comparison between common, commercially available insect repellents utilized in this study, the neat repellents DEET and picaridin as well as the insecticide permethrin, were first analyzed via TGA and profiles shown in Figure 3.

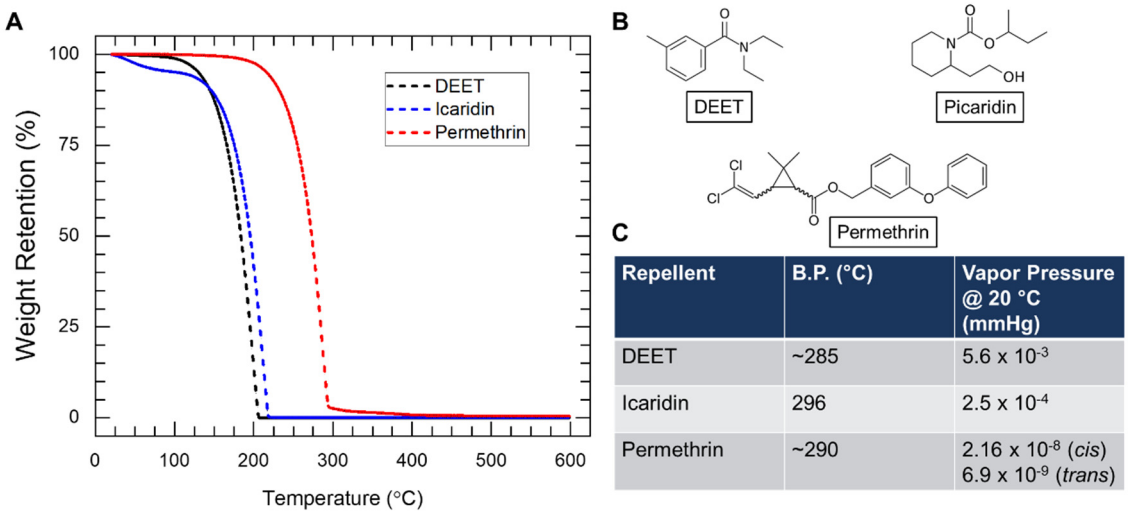

Repellent	B.P. (°C)	Vapor Pressure @ 20 °C (mmHg)
DEET	~285	5.6×10^{-3}
Icaridin	296	2.5×10^{-4}
Permethrin	~290	2.16×10^{-8} (*cis*) 6.9×10^{-9} (*trans*)

Figure 3. A) TGA, B) chemical structures, and C) physical properties of neat repellents.

The insect repellents DEET and picaridin are liquid at room temperature with boiling points of 285 °C and 296 °C, respectively, while permethrin is a crystalline solid at room temperature with a boiling point at 290 °C. With respect to the repellents, TGA profiles showed at significant loss of mass at ~125 and ~150 °C for DEET and picaridin, respectively. These temperatures are

well below their thermodynamic boiling points, indicating substantial loss of mass due to evaporation and increased vapor pressures with increasing temperature. This result is not necessarily unexpected as it is important for insect repellents to be semi-volatile in order to provide effective protection by interacting with olfactory senses of the aforementioned biting arthropods. Importantly, the mass loss temperatures from the TGA profiles in Figure 3 served as controls for subsequent comparison of repellent encapsulation in Nylon-6,6 nanofibers, explored in more depth below.

4.1. Monofilament Fiber Morphology and Composition

The effect of fiber composition on morphology was first investigated via scanning electron microscopy (SEM). Representative SEM images, shown in Figure 4, show that incorporation of DEET into Nylon-6,6 fibers had minimal effect on fiber morphology at relatively low (ND10, < 10 wt%) concentrations, while smaller fibers were observed in ND30 and ND50 fibers.

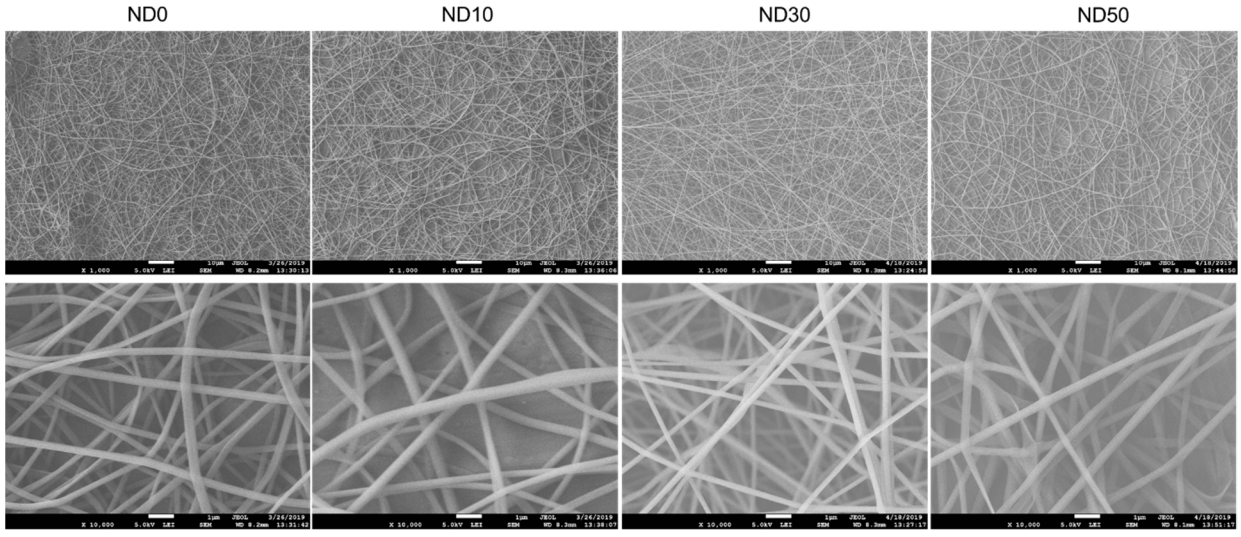

Figure 4. Scanning electron micrographs of monofilament ND composites. Representative scale bars for top and bottom are 20 μm and 2 μm, respectively.

The change in fiber size was attributed to a dilution effect of the addition of DEET into the formic acid/polymer solution. In all cases, the amount of formic acid as solvent used in each electrospinning solution was held constant, resulting in a dilution effect when liquid DEET repellent was incorporated. The result was the spinning of a solution with an effectively lower polymer concentration, which has been shown numerous times to result in a decrease in fiber diameter.

Electrospun repellent fibers were than analyzed thermally using thermagravimetric analysis (TGA) to identify fiber composition and isothermal release kinetics. Heating ramp profiles were used to identify the equilibrium composition upon heating to 300 °C (Figure 5), after all the repellent had evaporated from the fiber mat. It was observed that each fiber retained approximately half of the DEET dissolved in the original electrospinning solution, where ND10, ND30, and ND50 fibers contained 4.5, 12.5, and 25.5 wt% DEET, respectively. The loss of DEET was not completely unexpected, as DEET is a relatively volatile small-molecule that would be expected to partially evaporate, along with the volatile formic acid solvent, during the electrospinning process.

A

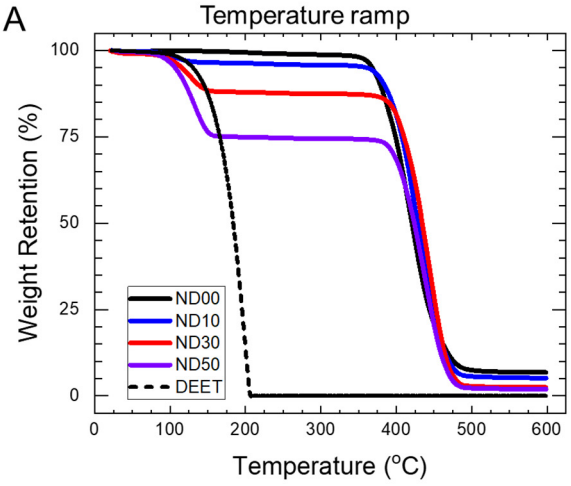

B

Sample	Composition (from TGA)
ND10	~4.5 wt%
ND30	~12.5 wt%
ND50	~25.5 wt%

Figure 5. A) TGA profiles for ND composite fibers and B) final wt% DEET composition.

The effect of DEET loading concentration on long-term release capability of electrospun ND fibers was evaluated by measuring DEET release at several elevated temperatures, from which ambient performance can be extrapolated. Relevant isothermal TGA profiles for ND10 composites at 60 and 80 °C are shown in Figure 6. The release rate of all samples increased with increasing temperature and increasing DEET loading. Further, at 80 and 100 °C, all DEET was released from the fibers and agreed well with the equilibrium loadings calculated from TGA heating ramps. However, at 60 °C, about half of the DEET remained in the fibers, compared to what would be expected based on compositions extracted from Figure 5. The most likely explanations for this observation are 1) the lower vapor pressure of DEET at lower temperature along with the physical Nylon-6,6 barrier resulted in efficient encapsulation of DEET in the fiber matrix and 2) the proximity to the glass transition temperature of Nylon-6,6, which is between 45 and 60 °C, where a glassy phase restricts small-molecule diffusion substantially compared to at elevated temperatures. This aids in the design of repellent fibers by considering the totality of both ambient environment (*i.e.* temperature) and materials properties when designing warfighter uniforms.

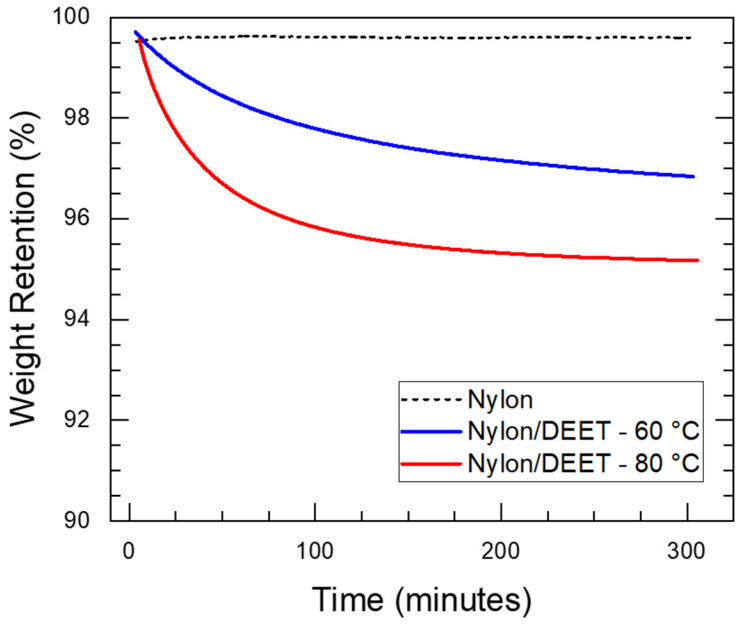

Figure 6. Isothermal TGA profiles for Nylon and ND10 at 60 and 80 °C.

5. Results and Discussion – Picaridin Fibers

Incorporation of the liquid repellent picaridin into solutions of Nylon-6,6 (structures shown in Figure 7) in formic acid, similarly to DEET, was expected to behave as a non-volatile diluent, homogenously distributed throughout the fiber matrix during the electrospinning process, resulting in a composition-dependent fiber morphology. After confirmation that Nylon/picaridin (NP) solutions were miscible over the composition range of interest, fiber morphology was analyzed.

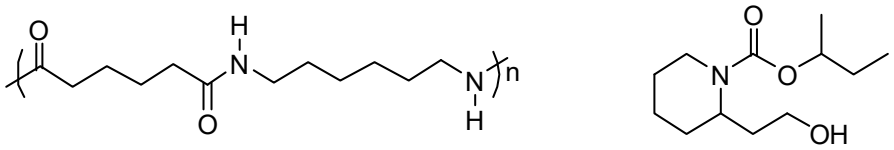

Figure 7. Chemical structures of Nylon 6,6 (left) and picaridin (right).

5.1. Monofilament Fiber Morphology and Composition

The effect of repellent content on fiber morphology was investigated with SEM. Representative scanning SEM images, in Figure 8, confirmed that all NP composite fibers were free of defects (e.g. globules, ill-defined shape, etc.) and able to be electrospun at all repellent compositions. Unloaded nylon fibers exhibited average fiber diameters of 279±76 nm. The morphology and size of nanofibers was largely unaffected by incorporation of picaridin even at extremely high (*i.e.* 50 wt%) loadings (Figure 9). This result was likely because the picaridin loading had minimal impact on the initial electrospinning polymer solution viscosity and dielectric properties, despite the significant weight contribution of picaridin to fibers after elelctrospinning. Importantly, picaridin loading did not have negative effects on morphology and size, thus potential development and use of such fibers for repellent textiles are not limited by picardin loading levels.

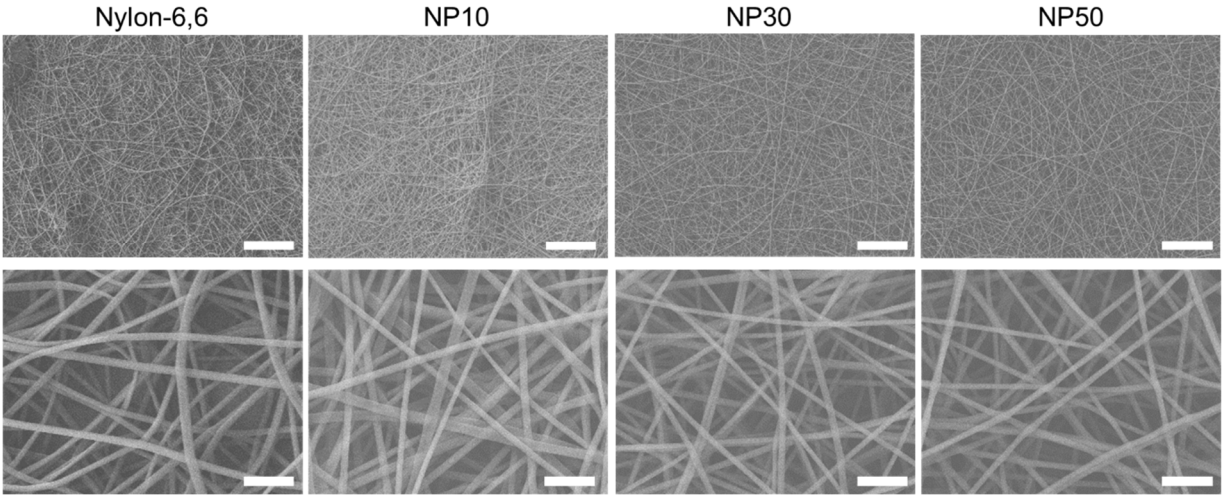

Figure 8. Scanning electron micrographs of monofilament NP composites. Representative scale bars for top and bottom are 20 μm and 2μm, respectively.

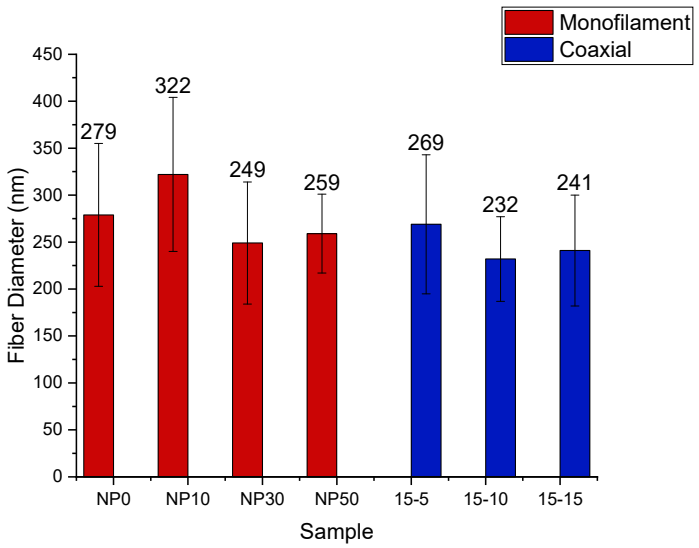

Figure 9. Average fiber diameters (± 1 standard deviation) of NP monofilament (red) and coaxial (blue) fibers.

The overall composition of electrospun nanofibers were evaluated using thermograviemtric analysis (TGA). First, TGA ramps were performed to elucidate the overall repellent composition of each of the fibers. Figure 10 shows TGA profiles for each of the NP composite fibers, where the weight loss of at temperatures less than 350 °C was attributed to loss of picaridin. A TGA ramp of pure picaridin is included for comparison. In each case, the experimentally determined picaridin loading was slightly less than the nominal solution concentration used during spinning, indicating that most of the picaridin loading was maintained during the electrospinning process. Discrepancy in these two values can be explained by the low, but non-negligible vapor pressure of picaridin (~3.3 x 10^{-2} Pa) at ambient conditions, that resulted in a portion of the liquid repellent being lost to evaporation during the spinning process.

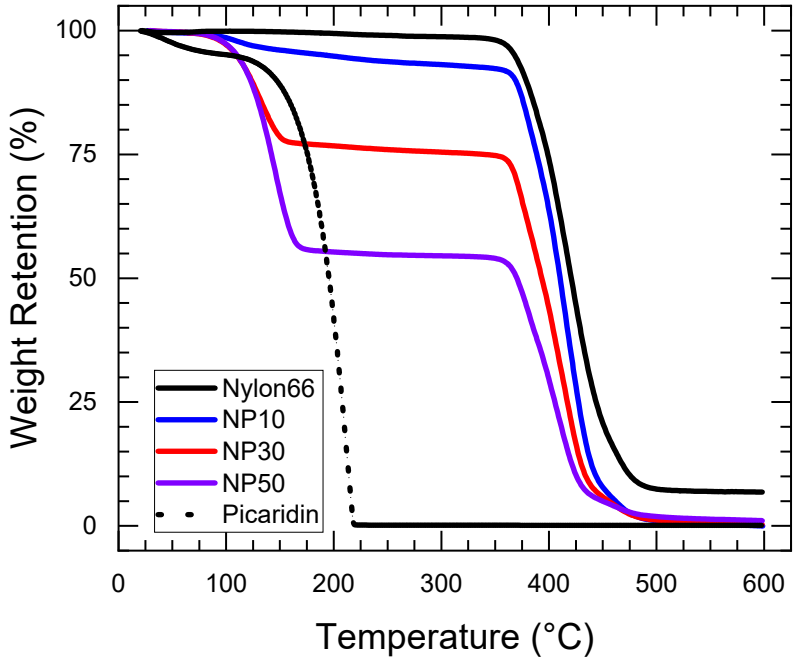

Figure 10. TGA profiles for NP composite fibers.

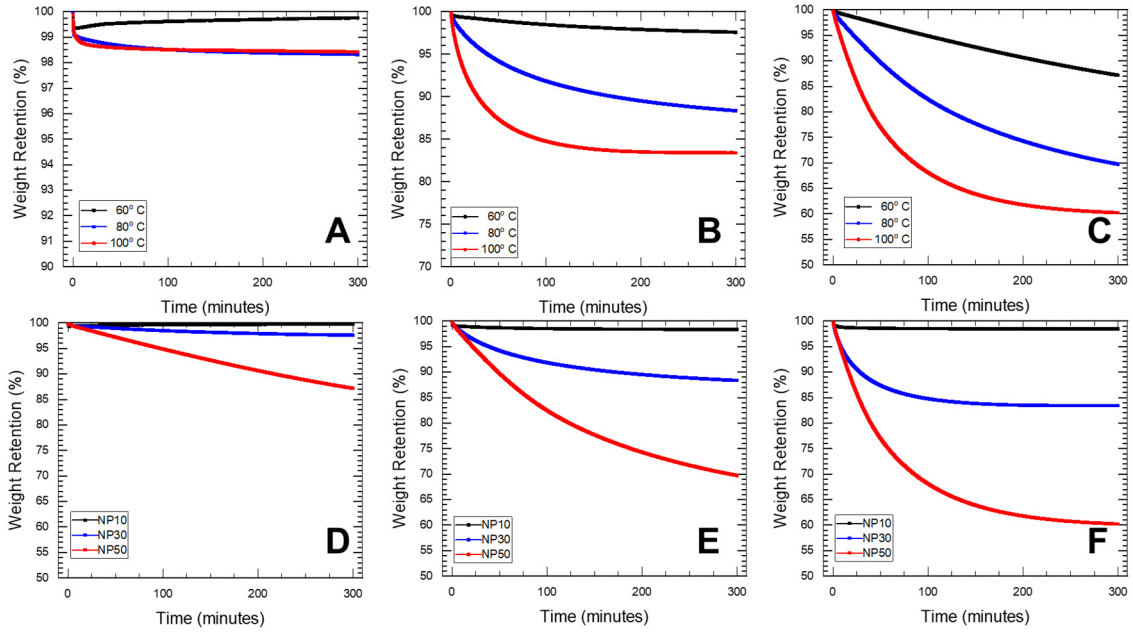

Figure 11. Isothermal TGA profiles for NP10 (A), NP30 (B), NP50 (C), and all NP composites at 60 °C (D), 80 °C (E), and 100 °C (F).

The effect of picaridin loading concentration on long-term release capability of electrospun NP fibers was evaluated by measuring picaridin release at several elevated temperatures, from which ambient performance can be extrapolated. Specifically, isothermal TGA experiments were performed for each of the fibers at 60, 80, and 100 °C to monitor the diffusion of picaridin from the fibers over time (Figure 11). Expectedly, the release rate of all samples increased with increasing temperature and increasing picaridin loading (Figure 11 A-C). Interestingly, none of the samples released all of the picaridin (noted by dashed horizontal line in Figure 11) after 300 min at 100 °C, demonstrating significant stability of the NP fibers as well as potential for long-term release capability at lower temperatures. Indeed, all samples continued to release picaridin at the maximum time measured, 300 min, even at 100 °C. In all cases, release profiles demonstrated exponential decay in weight retention, W_t, which corresponded to a first order loss of repellent with time that can be further modeled by a simple function of the form

$$W_t = W_0 \left(\exp\frac{-t}{\tau} + 1\right) \quad (1)$$

Where t is the time in minutes, W_0 is the initial weight, and τ is a time constant related to diffusion of picaridin through the electrospun nanofibers. Figure 12 depicts the time constant, τ, as a function of temperature for each of the NP composites. In general, extrapolation of time constants across the temperature range demonstrate linear agreement for each sample, except for NP50 at low (60° C) temperatures. This outlier was attributed to several underlying mechanisms that warrant further discussion. Since the fiber diameters for all fibers are statistically similar, there was no surface area effect difference between the samples. Therefore, differences in release profiles were likely due to differing concentration gradients resulting from increased picaridin

loading.

The inverse lifetime ($1/\tau$) was fit to an Arrhenius plot (Figure 12, right), from which the activation energy of insect repellent release for each NP composite was calculated from the relationship:

$$slope = \frac{-E_a}{2.3R}$$

Where E_a is the activation energy and R is the universal gas constant (8.314 J/K•mol). The activation energies for all NP composites fall within the range of 37-60 kJ/mol. NP10 and NP30 exhibited statistically similar activation energies. NP50 demonstrated slightly higher activation energy at 60±8 kJ/mol, which was attributed to the effect of the 60 °C lifetime value on the slope of the NP50 plot. Using the calculated activation energy, the behavior of each composite at ambient temperature, 20 °C, was extrapolated and resulted in half-lives ($t_{1/2}$) for release of 13.6, 13.0, and 132.7 h for NP10, NP30, and NP50, respectively.

In the case of each NP composite fiber, a simple assumption is made that the liquid repellent is homogenously dispersed/incorporated into the Nylon matrix resulting in a uniform composition throughout. At relatively low loadings (*i.e.* NP10) it is presumed that this to be a good assumption. However, because picaridin and Nylon-6,6 are not miscible, phase separation is expected to occur. At extremely high loadings of repellent (*i.e.* NP50), substantially more phase separation is expected to occur, due to physical confinement, resulting in a non-uniform dispersion of repellent within the polymer matrix. It is therefore anticipated that electrospinning results in a significantly higher repellent composition at the surface of the fiber compared to NP10 or NP30. Additionally, this repellent will inherently behave as a volatile, small-molecule diluent.

Consequently, the repellent closest to the surface will diffuse out of the matrix very quickly leaving behind a glassy surface that becomes much more difficult for the picaridin to diffuse through at temperatures below the glass transition temperature of the matrix, resulting in very long repellent lifetimes.

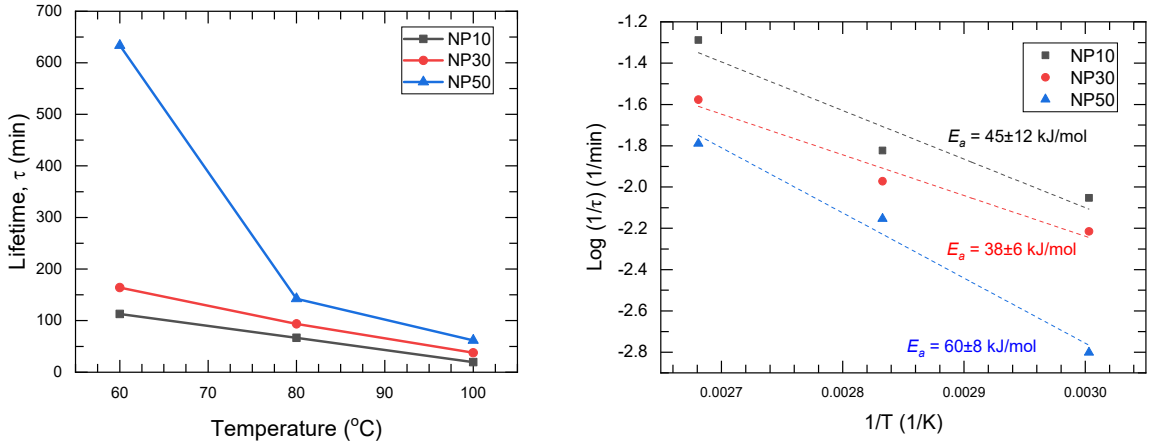

Figure 12. Lifetimes extracted from isothermal TGA plots using Eq. 1 (left) and Arrhenius plot showing calculated activation energy (E_a) (right).

5.2. Structural Analysis

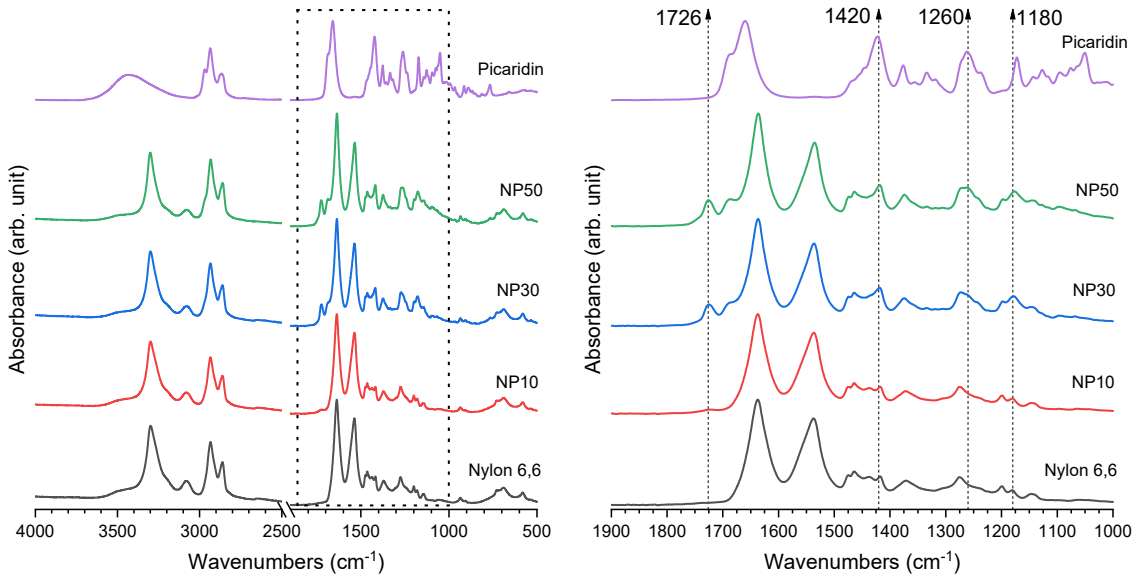

Figure 13. ATR-IR spectra of neat picaridin, neat Nylon, and NP composites showing full spectrum (left) and region of interest (right).

The structural composition of the NP fibers were evaluated with ATR-IR. Figure 1313 shows overlay of NP composite spectra as compared to pure Nylon-6,6 and picaridin. Neat picaridin exhibited characteristic broad absorbance at 3434 cm^{-1} from ν_s(OH), sharp peaks at 2934 and 2866 cm^{-1} corresponding asymmetric and symmetric CH_2 ($\nu_{as}(CH_2)$), respectively, a shoulder at 1690 cm^{-1} due carbamate carbonyl stretching (ν_s(C=O)), and a sharp peak at 1659 cm^{-1} from hydrogen bonded carbamate carbonyl stretch(ν_s(C=O)). Neat Nylon-6,6 demonstrated characteristic modes at 3300 cm^{-1} (ν_s(NH)), 3078 cm^{-1} (ν_s(HN-C=O)), 2932 and 2861 cm^{-1} corresponding asymmetric ($\nu_{as}(CH_2)$) and symmetric CH_2 ($\nu_s(CH_2)$), respectively, 1636 cm^{-1} from amide I carbonyl (ν_s(C=O)), 1536 cm^{-1} from amide II band (ν_s(HN-C=O)), and 1275 cm^{-1} attributed to the amide III band. Many of the strong absorbance bands of picaridin overlapped those of Nylon-6,6 due to similarity in shared functional groups (amide/carbamate and alkyl moieties, Figure 7). In fact, the NP composites fibers exhibited very similar absorbance to neat nylon-6,6 across most of the IR region, even at the highest (NP50) loading levels. The NH (3300 cm^{-1}) and CH_2 (2800-3000 cm^{-1}) regions were largely unaffected by picaridin loading. Surprisingly, there was no shift in the Nylon amide I carbonyl peak upon loading with picaridin, despite the carbamate carbonyl of picaridin absorbing at 1660 cm^{-1} compared to the amide carbonyl of Nylon-6,6 at 1636 cm^{-1}. Increased picaridin loading was confirmed by the increased intensity of several bands at 1690 cm^{-1} (ν_s(C=O)), 1423 cm^{-1} ($\delta(CH_2)$), 1262 cm^{-1} (ν_s(C-N)), and 1172 cm^{-1} (ν_s(C-O)),), all of which did not shift relative to neat picaridin. Thus, not only did the increase in these peaks confirm picaridin loading in the nylon fibers, but their lack of shift from neat picardin also indicated that there were minimal picaridin-nylon intermolecular interactions. Interestingly, the NP composites exhibited a

new peak in the carbonyl region at 1726 cm^{-1} that was attributed to small amounts of residual formic acid that remained due to stabilizing interactions with picaridin since the peak was not present in neat Nylon nor picaridin (Figure 13, right). Taken together, these results suggest that the majority of picaridin was physically entrapped within the nylon matrix. As such, release of picaridin from the monofilament nylon fibers would be expected to be dependent on diffusion of the picaridin insect repellent through the solid polymer matrix, relatively independent of intermolecular interactions.

Further investigation into interactions of Nylon-6,6 and picaridin via differential scanning calorimetry (DSC) showed that no appreciable mixing of the phases occurred. Figure 14 shows the first heating profiles of NP composites and no substantial differences in the melting endotherm, indicating immiscibility of the two phases. One interesting aspect of these profiles is the presence of two peaks between 250 and 275 °C in neat Nylon-6,6 that become less distinct with increasing picaridin loading. An explanation for this phenomena is most likely due to changes in the Nylon-6,6 crystal phase that has been shown previously as a result of both the spatial confinement as a result of small, nanoscale fibers in the presence of an anti-solvent.

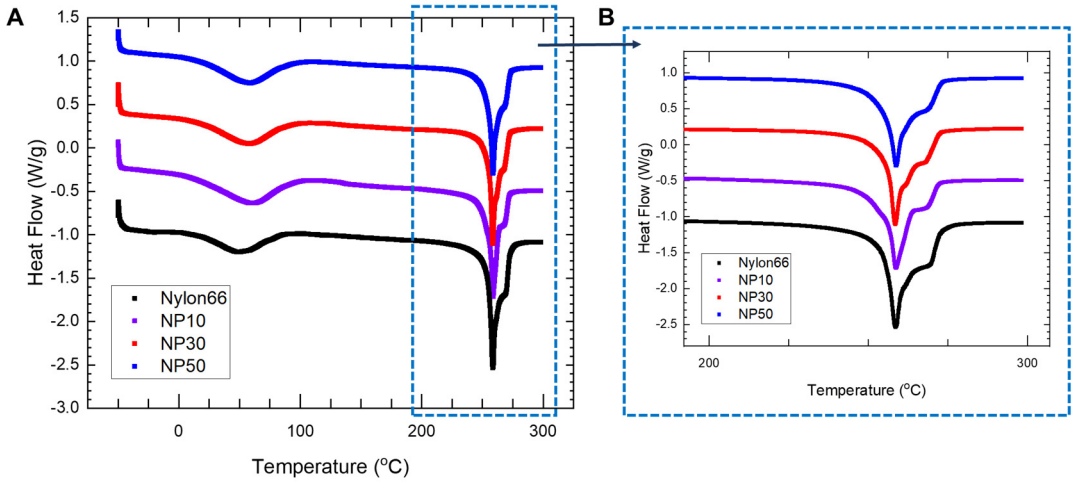

Figure 14. DSC analysis of NP composites.

5.3. Coaxial Fiber Morphology and Composition

In an effort to impart an additional level of control over release kinetics and provide a protective barrier to water exposure, coaxial fibers composed of a picaridin loaded nylon core and an unloaded nylon sheath were fabricated via coaxial electrospinning. Specifically, the amount of picaridin loading in the core was controlled by modifying the core solution flow rate (5, 10, and 15 μL/min), which was a picaridin/nylon solution. SEM was used to visualize the effect of coaxial electrospinning and picaridin loading in the core on fiber morphology (Figure 15). Fibers were formed in all cases, though a noticeable increase in defects (*i.e.* beads) was observed, especially at high core flow rates. This increase in defects is most likely due to the total mass flow exiting the needle tip to be greater than the optimal flow rate, that has been shown to produce beaded fibers from reduced charge density.[27] The fiber diameters of coaxial fibers were similar to those of the monofilament fibers in the range of 230-270 nm (Figure 9). Furthermore, average coaxial fiber diameter was also unaffected by core flow rate. Therefore, all fiber samples exhibited comparable surface area to volume ratios such that differences in release rate were attributed to loading composition and morphology (monofilament vs. coaxial).

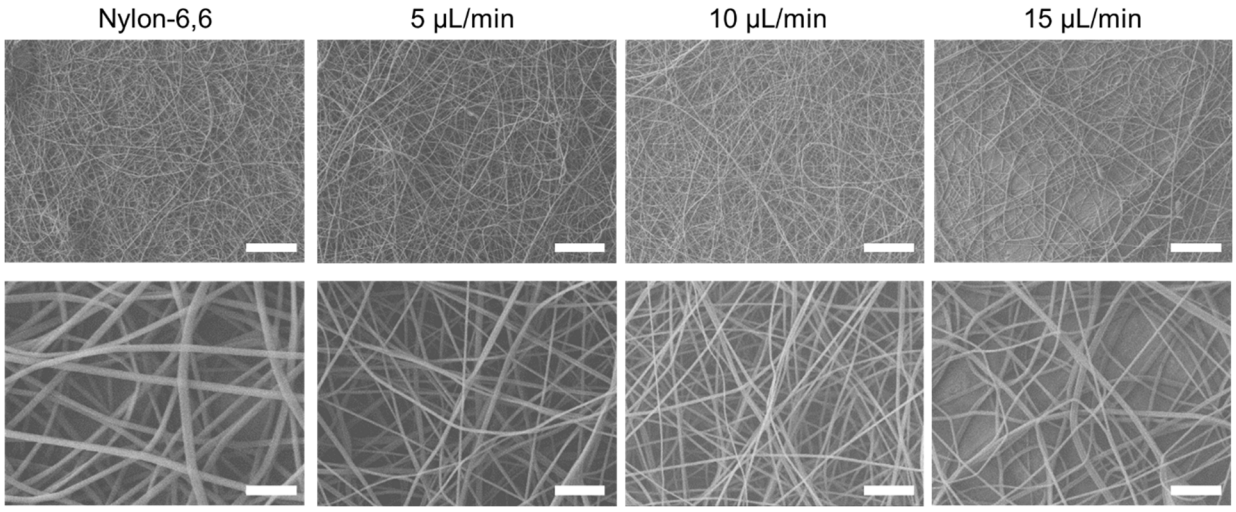

Figure 15. Scanning electron micrographs of coaxial NP composites. NP composties were spun at constant sheath flow rates of 15 µL/min and variable core flow rates of 5, 10, and 15 µL/min. Representative, scale bars for top and bottom are 20 µm and 2µm, respectively.

Repellent composition of the coaxial fibers was determined by TGA. Figure 16 shows TGA heating ramps profiles for all coaxial samples. The first noticeable difference between the coaxial and monofilament profiles is the presence of two regions of mass loss, at ~150 and ~200 °C. Additionally, in the case of the coaxial Nylon-6,6 control, mass loss was also observed at ~200° C that was not observed in the case of the monofilament control (Figure S1). As such, this mass loss was attributed to trapped residual solvent (formic acid) in the core of the hybrid coaxial Nylon structure, suggesting that the mass loss at lower (~150° C) temperature was due to incorporation of picaridin. This is surprising since the monofilament fibers, particularly neat Nylon-6,6 fibers, did not exhibit this behavior. Therefore, coaxial electrospinning of nylon/nylon coaxial fibers imparted some barrier properties that reduced the amount of solvent from evaporating from the core of the fibers during electrospinning. Further analysis of the TGA profiles showed a systematic increase in picaridin composition with increasing core flow rate, demonstrating the ability to tune fiber composition in a simple manner. Indeed, the approximate nominal wt% loadings of the coaxial fibers were 3.5, 5.0, and 10.8 wt% for the 15-5, 15-10, and 15-15 coaxial fibers,

respectively. Notably, the 15-15 coaxial fibers were comparable in loading concentration to the NP10 monofilament fibers as both were approximately 10 wt% picardin.

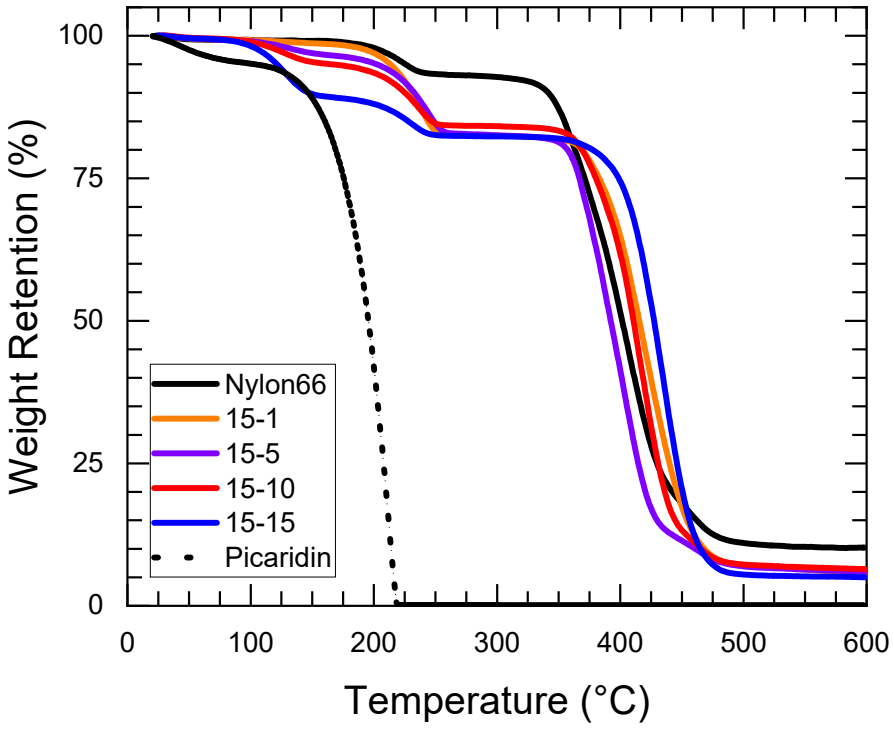

Figure 16. TGA ramp profiles for coaxial nanofiber composites.

6. Comparison of DEET and Picaridin Fibers

Overall incorporation of both DEET and picaridin into Nylon-6,6 nanofibers resulted in homogeneous repellent dispersion and incorporation dependent upon the repellent vapor pressure. Ultimately, composites resulting from electrospun solutions of DEET/Nylon-6,6 retained significantly less repellent than that of solutions containing picaridin/Nylon-6,6. Figure 17 shows the repellent compositions and heating ramp TGA profiles for electrospun nanofibers that were largely dependent on the equilibrium vapor pressure of the neat insect repellent. Encapsulation of picaridin was significantly more efficient compared to DEET due to a vapor pressure nearly one order of magnitude lower.

The similarity in fiber morphology is also indicative of the homogeneous distribution of liquid repellents that does not impede fiber formation. As shown in the coaxial NP fibers, high core flow rates resulted in fibers containing substantially more defects due to the large amount of solvent used during electrospinning. One would expect a similar result for monofilament fibers at comparably high repellent loadings (*i.e.* >> 50wt%) and/or low polymer concentration in solution.

Additionally, the difference in compositions obtained during electrospinning could be further characterized by looking at mixed repellent systems. Based on SEM images of each of the monofilament ND and NP composites, it would be expected that utilizing a mixed repellent system would result in fiber morphologies similar to that of the neat composites, but with tunable fiber composition and release profiles.

A

Sample	Composition (from TGA)
ND10	~4.5 wt%
ND30	~12.5 wt%
ND50	~25.5 wt%

B

Sample	Composition (from TGA)
NP10	~6.8 wt%
NP30	~25.5 wt%
NP50	~45.5 wt%

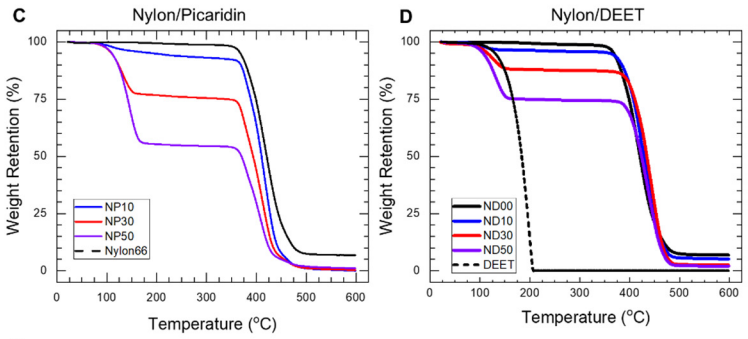

E

Repellent	Vapor Pressure @ 20 °C (mmHg)
DEET	5.6×10^{-3}
Picaridin	2.5×10^{-4}

Figure 17. Equilibrium repellent compositions of electrospun fibers containing (A) DEET and (B) picaridin from isothermal TGA profiles. Compositions were extracted from heating ramp TGA profiles for NP (C) and ND (D) composites at 300° C. Equilibrium vapor pressures (E) for each repellent were partially responsible for the overall amount of repellent incorporated into electrospun nanofibers.

7. Summary and Conclusions

Repellent nanofibers composed of picaridin in Nylon-6,6 were successfully developed. A comparison of fiber morphology on release behavior was performed between monofilament and coaxial fibers. Monofilament composites with varying repellent concentrations were prepared and release rates were tuned and characterized via isothermal TGA. Coaxial fibers were then developed and TGA demonstrated that the outer protective sheath altered the release of volatile components. Expectedly, the release rate of all samples increased with increasing temperature and increasing picaridin loading. Importantly, fiber morphology and size was maintained with picaridin loading. Further, the NP fibers exhibited significant stability and potential for long-term release capability at ambient conditions since all composites continued to release picaridin even after 300 min at 100 °C. Picaridin was physically entrapped in the nylon matrix, exhibiting minimal picaridin-nylon intermolecular interactions, thus indicating that differences in release profiles were likely due to differing concentration gradients dependent on diffusion through the solid polymer matrix.

Additionally, coaxial electrospun nylon/nylon coaxial fibers imparted barrier properties that reduced the amount of solvent from evaporating from the core of the fibers during electrospinning. Overall, this work demonstrates a facile method to fabricate nylon fibers with controlled release kinetics of insect repellent. Furthermore, the coaxial designs employed via electrospinning herein have the potential to be employed using conventional fiber drawing techniques. As such, the results of this work have potential to enable a new approach to textile manufacture to generate numerous multifunctional products that could impact multiple applications, including intelligently designed 'smart' uniforms garments with localized behavior (e.g. collars with high loading of insect repellent).

8. Implications for Continued Research and Applications

The results of this work demonstrate a proof of concept of electrospinning as an effective method to encapsulation insect repellent and modulate release behavior. As such, this work demonstrates potential for continued work in the following focus areas:

8.1. Coaxially Designed Insect repellent yarns and fabrics

The successful results presented above demonstrates potential for continued research into insect repellent fibers, yarns, and fabrics. Several potential paths are briefly described below.

Mixed repellent systems. Coaxial electrospinning can be employed to fabricate composite fibers containing two different insect repellents, i.e. DEET and picaridin, in a single fiber. Based on SEM images of each of the monofilament ND and NP composites, it would be expected that utilizing a mixed repellent system would result in fiber morphologies similar to that of the neat composites, but with tunable fiber composition and release profiles. Furthermore, the release profiles of insect repellents with different vapor pressure could be tuned to enable complementary release profiles to leverage potential synergistic effects in repellency.

Electrospun Yarns. Picaridin/Nylon fibers in the form of a tow from electrospinning will be mechanically twisted into thread and yarn prototypes using an established technique that employs a funnel shaped electrospinning target. The final deliverable will be prototype threads that exhibit insect repellent and/or fire retardant properties (depending on which individual nano-/micro-fibers are used) with comparable mechanical properties of traditional polymer-based yarns. Such yarns would have potential to be incorporated into textiles through conventional weaving methods and provide the flexibility to be used only where needed in the garment.

Transition to Conventional Fiber Fabrication. Following the demonstration of

functionality of the core-shell fiber approach has been demonstrated using the low material requirements and flexible processing controls afforded by electrospinning, the technology will be further developed using melt extrusion techniques. The materials envisioned here for textiles are compatible with melt extrusion and fiber drawing technology, which will be a key transition path for the core-shell fiber morphology. Demonstrating similar performance from a melt-processed fiber compared to the electro-spun product would enable a large enhancement in fiber production rate (from g/hr to kg/hr) and be amenable to textile production through loom techniques.

8.2. Encapsulation of Flame Retardants, Antimicrobial, and Other Functional Additives

The results from this study demonstrate a facile approach to encapsulate and fabricate nanostructured textiles with volatile and non-volatile additives that could be easily adapted to the encapsulation of other functional components. Of particular potential interest is for development of flame-retardant textile for uniforms. Utilizing a similar approach as to that of repellent fibers, flame retardants incorporated into polymer solutions can be produced and tested using a variety if MIL-STD. The number and application area of functional additives is immense and has the potential to be a ripe area for both fundamental research and technology transition.

New functional fibers have potential to achieve improved performance with lower loading levels of active components than current uniforms, thus reducing the safety, health, and environmental burden of the textiles. Furthermore, electrospinning can serve as a testbed technology to allow for rapid prototype and demonstration of the coaxial designs, from which more conventional coaxial processing techniques can be easily adapted for transition to large scale production.

References

1. Katz, T. M.; Miller, J. H.; Hebert, A. A., Insect repellents: Historical perspectives and new developments. *Journal of the American Academy of Dermatology* **2008,** *58* (5), 865-871.
2. Tavares, M.; da Silva, M. R. M.; de Oliveira de Siqueira, L. B.; Rodrigues, R. A. S.; Bodjolle-d'Almeida, L.; dos Santos, E. P.; Ricci-Júnior, E., Trends in insect repellent formulations: A review. *International Journal of Pharmaceutics* **2018,** *539* (1), 190-209.
3. DeGennaro, M., The mysterious multi-modal repellency of DEET. *Fly* **2015,** *9* (1), 45-51.
4. Swale, D. R.; Sun, B.; Tong, F.; Bloomquist, J. R., Neurotoxicity and Mode of Action of N, N-Diethyl-Meta-Toluamide (DEET). *PLOS ONE* **2014,** *9* (8), e103713.
5. Drakou, C. E.; Tsitsanou, K. E.; Potamitis, C.; Fessas, D.; Zervou, M.; Zographos, S. E., The crystal structure of the AgamOBP1•Icaridin complex reveals alternative binding modes and stereo-selective repellent recognition. *Cellular and Molecular Life Sciences* **2017,** *74* (2), 319-338.
6. Klun, J. A.; Khrimian, A.; Debboun, M., Repellent and Deterrent Effects of SS220, Picaridin, and Deet Suppress Human Blood Feeding by Aedes aegypti, Anopheles stephensi, and Phlebotomus papatasi. *Journal of Medical Entomology* **2006,** *43* (1), 34-39.
7. Büchel, K.; Bendin, J.; Gharbi, A.; Rahlenbeck, S.; Dautel, H., Repellent efficacy of DEET, Icaridin, and EBAAP against Ixodes ricinus and Ixodes scapularis nymphs (Acari, Ixodidae). *Ticks and Tick-borne Diseases* **2015,** *6* (4), 494-498.
8. Diaz, J. H., Chemical and Plant-Based Insect Repellents: Efficacy, Safety, and Toxicity. *Wilderness & Environmental Medicine* **2016,** *27* (1), 153-163.
9. Peila, R.; Scordino, P.; Shanko, D. B.; Caldera, F.; Trotta, F.; Ferri, A., Synthesis and characterization of β-cyclodextrin nanosponges for N,N-diethyl-meta-toluamide complexation and their application on polyester fabrics. *React. Funct. Polym.* **2017,** *119*, 87-94.
10. Annandarajah, C.; Norris, E. J.; Funk, R.; Xiang, C.; Grewell, D.; Coats, J. R.; Mishek, D.; Maloy, B., Biobased plastics with insect-repellent functionality. *Polymer Engineering & Science* **2019,** *59* (s2), E460-E467.
11. Faulde, M. K.; Albiez, G.; Nehring, O., Insecticidal, acaricidal and repellent effects of DEET- and IR3535-impregnated bed nets using a novel long-lasting polymer-coating technique. *Parasitology Research* **2010,** *106* (4), 957-965.
12. Place, L. W.; Gulcius-Lagoy, S. M.; Lum, J. S., Preparation and characterization of PHMB-based multifunctional microcapsules. *Colloids and Surfaces A: Physicochemical and Engineering Aspects* **2017,** *530* (Supplement C), 76-84.
13. Gomes, G. M.; Bigon, J. P.; Montoro, F. E.; Lona, L. M. F., Encapsulation of N,N-diethyl-meta-toluamide (DEET) via miniemulsion polymerization for temperature controlled release. *J. Appl. Polym. Sci.* **2019,** *136* (9), 47139.

14. Akbarzadeh, A.; Mokhtari, J.; Kolkoohi, S.; Amin Sarli, M., Imparting insect repellency to nylon 6 fibers by means of a novel MCT reactive dye. *J. Appl. Polym. Sci.* **2012,** *126* (3), 1097-1104.

15. Luo, C. J.; Stoyanov, S. D.; Stride, E.; Pelan, E.; Edirisinghe, M., Electrospinning versus fibre production methods: from specifics to technological convergence. *Chem. Soc. Rev.* **2012,** *41* (13), 4708-4735.

16. Lundin, J. G.; Coneski, P. N.; Fulmer, P. A.; Wynne, J. H., Relationship between surface concentration of amphiphilic quaternary ammonium biocides in electrospun polymer fibers and biocidal activity. *Reactive and Functional Polymers* **2014,** *77*, 39-46.

17. Bischel, L. L.; Coneski, P. N.; Lundin, J. G.; Wu, P. K.; Giller, C. B.; Wynne, J.; Ringeisen, B. R.; Pirlo, R. K., Electrospun gelatin biopapers as substrate for in vitro bilayer models of blood−brain barrier tissue. *Journal of Biomedical Materials Research Part A* **2016,** *104* (4), 901-909.

18. Bertocchi, M. J.; Simbana, R. A.; Wynne, J. H.; Lundin, J. G., Electrospinning of Tough and Elastic Liquid Crystalline Polymer–Polyurethane Composite Fibers: Mechanical Properties and Fiber Alignment. *Macromolecular Materials and Engineering* **2019,** *304* (8), 1900186.

19. Bonadies, I.; Longo, A.; Androsch, R.; Lorenzo, M. L. D., Electrospun fibers of poly(l-lactic acid) containing DEET. *AIP Conference Proceedings* **2018,** *1981* (1), 020112.

20. Bonadies, I.; Longo, A.; Androsch, R.; Jehnichen, D.; Göbel, M.; Di Lorenzo, M. L., Biodegradable electrospun PLLA fibers containing the mosquito-repellent DEET. *European Polymer Journal* **2019,** *113*, 377-384.

21. Cecone, C.; Caldera, F.; Trotta, F.; Bracco, P.; Zanetti, M., Controlled Release of DEET Loaded on Fibrous Mats from Electrospun PMDA/Cyclodextrin Polymer. *Molecules* **2018,** *23* (7), 1694.

22. Yarin, A. L., Coaxial electrospinning and emulsion electrospinning of core–shell fibers. *Polym. Adv. Technol.* **2011,** *22* (3), 310-317.

23. Bertocchi, M. J.; Ratchford, D. C.; Casalini, R.; Wynne, J. H.; Lundin, J. G., Electrospun Polymer Fibers Containing a Liquid Crystal Core: Insights into Semi-Flexible Confinement. *The Journal of Physical Chemistry C* **2018**.

24. Bertocchi, M. J.; Vang, P.; Balow, R. B.; Wynne, J. H.; Lundin, J. G., Enhanced Mechanical Damping in Electrospun Polymer Fibers with Liquid Cores: Applications to Sound Damping. *ACS Applied Polymer Materials* **2019,** *1* (8), 2068-2076.

25. Ghorani, B.; Tucker, N., Fundamentals of electrospinning as a novel delivery vehicle for bioactive compounds in food nanotechnology. *Food Hydrocolloids* **2015,** *51*, 227-240.

26. Sibanda, M.; Focke, W.; Braack, L.; Leuteritz, A.; Brünig, H.; Tran, N. H. A.; Wieczorek, F.; Trümper, W., Bicomponent fibres for controlled release of volatile mosquito repellents. *Materials Science and Engineering: C* **2018,** *91*, 754-761.

27. Fong, H.; Chun, I.; Reneker, D. H., Beaded nanofibers formed during electrospinning. *Polymer* **1999,** *40* (16), 4585-4592.

28. Babapoor, A.; Karimi, G.; Golestaneh, S. I.; Mezjin, M. A., Coaxial electro-spun PEG/PA6 composite fibers: Fabrication and characterization. *Applied Thermal Engineering* **2017,** *118*, 398-407.

29. Chen, C.; Zhao, Y.; Liu, W., Electrospun polyethylene glycol/cellulose acetate phase change fibers with core–sheath structure for thermal energy storage. *Renewable Energy* **2013,** *60*, 222-225.

30. Forward, K. M.; Flores, A.; Rutledge, G. C., Production of core/shell fibers by electrospinning from a free surface. *Chemical Engineering Science* **2013,** *104*, 250-259.

31. Hu, W.; Yu, X., Encapsulation of bio-based PCM with coaxial electrospun ultrafine fibers. *RSC Advances* **2012,** *2* (13), 5580-5584.

32. Li, D.; McCann, J. T.; Xia, Y., Use of Electrospinning to Directly Fabricate Hollow Nanofibers with Functionalized Inner and Outer Surfaces. *Small* **2005,** *1* (1), 83-86.

33. Lu, S.; Duan, X.; Han, Y.; Huang, H., Silicone rubber/polyvinylpyrrolidone microfibers produced by coaxial electrospinning. *Journal of Applied Polymer Science* **2013,** *128* (4), 2273-2276.

34. Zhang, H.; Qin, X.; Wu, J.; He, Y.-B.; Du, H.; Li, B.; Kang, F., Electrospun core–shell silicon/carbon fibers with an internal honeycomb-like conductive carbon framework as an anode for lithium ion batteries. *Journal of Materials Chemistry A* **2015,** *3* (13), 7112-7120.

35. Mapossa, A. B.; Sibanda, M. M.; Sitoe, A.; Focke, W. W.; Braack, L.; Ndonyane, C.; Mouatcho, J.; Smart, J.; Muaimbo, H.; Androsch, R.; Loots, M. T., Microporous polyolefin strands as controlled-release devices for mosquito repellents. *Chemical Engineering Journal* **2019,** *360*, 435-444.

36. Nerio, L. S.; Olivero-Verbel, J.; Stashenko, E., Repellent activity of essential oils: A review. *Bioresource Technology* **2010,** *101* (1), 372-378.

37. Place, L. W.; Gulcius-Lagoy, S. M.; Lum, J. S., Preparation and characterization of PHMB-based multifunctional microcapsules. *Colloids and Surfaces A: Physicochemical and Engineering Aspects* **2017,** *530*, 76-84.

38. Bertocchi, M. J.; Ratchford, D. C.; Casalini, R.; Wynne, J. H.; Lundin, J. G., Electrospun Polymer Fibers Containing a Liquid Crystal Core: Insights into Semiflexible Confinement. *The Journal of Physical Chemistry C* **2018,** *122* (29), 16964-16973.